RSC Advances

PAPER

View Article Online
View Journal | View Issue

Cite this: *RSC Adv.*, 2021, **11**, 12641

Facile construction of a family of supramolecular gels with good levofloxacin hydrochloride loading capacity†

Renyuan Chen,[a] Caidie Xu,[a] Yihao Lei,[a] Hongxin Liu, *[b] Yabin Zhu, [c] Jianfeng Zhang[a] and Long Xu *[a]

Received 30th January 2021
Accepted 15th March 2021

DOI: 10.1039/d1ra00809a

rsc.li/rsc-advances

Due to their designability and easy functionalization (such as self-antimicrobial, high antibiotic loading content, injectable, and sustained drug release), low molecular weight gels have attracted significant attention as antimicrobial materials. Herein, a series of biocompatible low molecular weight gelators (LMWGs) were designed and synthesized, using dihydrazides with different alkyl chains, which show excellent gelation ability in PEG200 and PEG400. Among these gelators, a low molecular weight hydrogelator (LMWH) was obtained by introducing an appropriate length of the alkyl chain. The supramolecular gels exhibited good shear thinning behavior, destruction–recovery ability, and excellent antibiotic (levofloxacin hydrochloride) loading capacity (as high as 66.7%). FT-IR and ^{1}H NMR were used for the investigation of the gelation process of gelators. Results suggest that regulating and controlling the balance of the hydrophilic and hydrophobic parts of the gelator structure by introducing different alkyl chain lengths is an effective method for constructing LMWHs.

1 Introduction

Recently, the application of supramolecular gels in many fields has been receiving increasing attention, including sensors, cosmetics, oil–water separation, cell culture, drug delivery, and tissue engineering.[1–4] Low molecular weight gelators (LMWGs) self-assemble into supramolecular gels by non-covalent physical interactions (such as hydrogen bonding, π–π stacking, van der Waals forces, and dipole–dipole interactions) in specific solvents.[5–7] LMWGs can be classified into low molecular weight organogelators (LMOGs) and low molecular weight hydrogelators (LMWHs) based on the medium, in which (organic solvent or water) they form the gel. Due to their easy synthesis, high tunability and dynamic/responsive properties, supramolecular gels have distinct advantages as compared to the widely used polymer-based gels.[8–10]

Microbial contamination is one of the major threats to human health globally. Great effort has been devoted to developing antimicrobial materials such as photosensitizers, Ag nanoparticles and antimicrobial hydrogels.[11–14] Due to the superior properties of high water retention ability, biocompatibility as well as biodegradability, supramolecular hydrogels have been widely used in biomedical fields such as antimicrobial therapy, wound healing, 3D-bioprinting, tissue engineering, drug delivery, and cancer therapy.[15–18] A lot of advanced antimicrobial hydrogels have been constructed, each with unique traits such as high water retention, enhanced biocompatibility, high oxygen permeability, excellent drug/antibiotic loading and releasing properties.[14] Antimicrobial hydrogels are widely used in wound healing, medical implant coatings, and infection treatment.[19–21] Adams *et al.* developed a supramolecular hydrogel and found that the antimicrobial activity and formation process of the hydrogel can be adjusted by the autoxidation of dopamine.[22] Kumar *et al.* prepared a series of anthranilamide-based hydrogels that showed antibacterial activity against *S. aureus*.[23] Tang *et al.* constructed a supramolecular hydrogel based on an amino acid-modified conjugated oligomer, which exhibited efficient capture and specific killing properties toward antibiotic-resistant bacteria.[24]

Despite many efforts that have been devoted to developing functionalized supramolecular hydrogels, unfortunately, the ideal LMWH is usually not easy to obtain. LMWHs are usually amphiphilic molecules, especially bolaamphiphiles. Barthélémy *et al.* constructed an injectable supramolecular hydrogel by bolaamphiphiles for selective sustained-release biomolecules.[25,26] Dong *et al.* constructed a bolaamphiphile using hydrophilic benzo-21-crown-7 and hydrophobic

[a]*Key Laboratory of Advanced Mass Spectrometry and Molecular Analysis of Zhejiang Province, School of Materials Science and Chemical Engineering, Ningbo University, Ningbo, 315211, China. E-mail: xulong@nbu.edu.cn*

[b]*College of Chemistry and Materials Engineering, Wenzhou University, Wenzhou, 325027, China. E-mail: hongxin-107@163.com*

[c]*Medical School of Ningbo University, Ningbo 315211, China*

† Electronic supplementary information (ESI) available: Table of critical gel concentrations and gelation behaviors of gelator in different solvents, ^{1}H NMR and ^{13}C NMR spectra of intermediate products and gelators. See DOI: 10.1039/d1ra00809a

tetrafluorobenzene, which self-assembled into a supramolecular hydrogel with lower critical solution temperature behavior.[27] Alonso *et al.* developed a series of bolaamphiphiles and explored their gelation performance and unraveled the key interactions for forming hydrogels by computational techniques.[28] It is commonly accepted that obtaining LMWHs requires a delicate balance between the hydrophilic and hydrophobic parts of the gelator structure, and controlling the hydrophobic interaction of the gelator is the key to designing LMWHs.[29] By taking advantage of the alkyl chain length to change the gelation properties and gel structure, the kinetics of supramolecule polymerization has been widely investigated.[30–32] To the best of our knowledge, using the length of the alkyl chain to adjust the balance of hydrophilic and hydrophobic parts of bolaamphiphiles for constructing LMWHs is rarely reported.

Numerous hydrazide compounds and their derivatives are bioactive molecules with antimicrobial and anti-inflammatory properties.[33,34] Since hydrazide groups easily form intermolecular hydrogen bonds, hydrazide compounds are potentially excellent gelators.[35,36] Biocompatible phenylalanine has been frequently used for constructing supramolecular gels.[37,38] The intense hydrogen bonding and π–π stacking interactions present in the phenylalanine sections make self-assembly easy.[39] Excitingly, supramolecular hydrogels based on phenylalanine showed antibacterial activity against Gram-negative bacteria by the combined effect of oxidative stress and membrane destruction.[40,41] Marchesan *et al.* constructed an antimicrobial hydrogel using a phenylalanine derivative.[42] Feng *et al.* developed phenylalanine-based chiral co-assembled hydrogels with enhanced mechanical properties and antimicrobial activity, which were prepared using a phenylalanine derivative and a dihydrazide compound.[43] To the best of our knowledge, simultaneously taking advantage of phenylalanine and hydrazide groups to construct LMWGs for antimicrobial therapy has not been reported.

In this study, a family of biocompatible bolaamphiphiles (LMWGs) was designed and synthesized, which showed excellent gelation ability in PEG200, PEG400, and a mixture of PEG200 and deionized water. The bolaamphiphiles (**2a**, **2b**, **2c**, **2d**, **2e**, **2f**) were facilely constructed by conjugating L-phenylalanine methyl ester to an aliphatic diacid or aliphatic diacid chloride, then reacting with hydrazine hydrate (Scheme 1). The hydrophobic phenyl groups and alkyl chains drive the self-assembly of LMWGs by π–π stacking and van der Waals forces, respectively. The hydrophilic hydrazide group facilitates LMWGs self-assembly by intermolecular hydrogen bonding. Gelation performance, mechanical strength, and balance of the hydrophilic and hydrophobic parts of the gelator structure were regulated by changing the length of the alkyl chain. The delicate balance between the hydrophilic and hydrophobic parts of compound **2d** was obtained by introducing the appropriate length of the alkyl chain, which resulted in compound **2d** being an effective hydrogelator (Scheme 2). Gelation mechanisms were studied by ^{1}H NMR spectra and FT-IR spectroscopy. The gel exhibited shear thinning behavior and destruction–recovery properties, which indicated that it is suitable for use in injectable gels. The gel also showed excellent antibiotic loading capacity and has great potential for application as an antimicrobial gel.

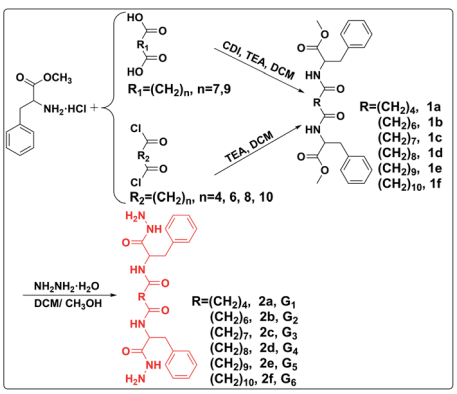

Scheme 1 A synthetic scheme showing low molecular weight gelators.

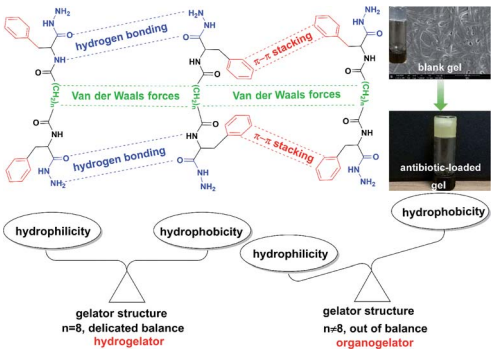

Scheme 2 The illustration of the self-assembly mechanism of the low molecular weight gel, and the key factor and effective ways for constructing a low molecular weight hydrogelator.

2 Results and discussion

2.1 Synthesis and characterization of target gelators

Bolaamphiphiles (compound **2**) as target gelators were prepared and characterized by ^{1}H NMR, ^{13}C NMR spectra and HRMS. The bolaamphiphiles were obtained by two steps of reaction. A lipophilic diester (compound **1**) was synthesized by conjugating L-phenylalanine methyl ester to both ends of the diacid ($HOOC(CH_2)_nCOOH$, $n = 7, 9$) or diacid chloride ($ClOC(CH_2)_n$-$COCl$, $n = 4, 6, 8, 10$). Bolaamphiphiles were obtained by the ammonolysis reaction of the diester and hydrazine hydrate. The peak that appeared near 2.16 ppm was the characteristic peak of the methylene connected to the carbonyl (–NHCOCH_2–), which indicated that the condensation reaction proceeded successfully. The other peaks in the spectra also matched the structure of compound **1** (Fig. S4–S14†). The results demonstrated that compound **1** was successfully prepared. The characteristic peak of the methoxy group disappeared and a new peak appeared for the amino group near 4.22 ppm (–CONHNH_2) in the spectrum of compound **2**, which proved that bolaamphiphiles were

obtained (Fig. S15–S25†). The ^{13}C NMR spectrum and HRMS also proved the correctness of the structure.

2.2 Gel characterizations

The gelation performances of bolaamphiphiles (**2a**, **2b**, **2c**, **2d**, **2e**, **2f**) with different lengths of alkyl chain were tested in 17 solvents with a wide range of polarities. Some of the gels are shown in Fig. 1. The gel photos of **2a** and **2b** are shown in Fig. S1.† Critical gel concentrations (CGC) of **2a**, **2b**, **2c**, **2d**, **2e**, and **2f** in different solvents are shown in Table S1.† All bolaamphiphiles (**2a**, **2b**, **2c**, **2d**, **2e**, **2f**) can form gels in PEG200 and PEG400, since the bolaamphiphile molecules in PEG solvent can achieve a balance between molecular dissolution and molecular aggregation. **2b**, **2c**, **2d**, **2e**, **2f** can also form gels in the mixed solvents of PEG200 and H_2O. **2d** can form gels in a variety of solvents, showing the best gelling performance. Excitingly, in this study we found that gelator **2d** ($n = 8$) can self-assemble into a hydrogel in a very low and narrow concentration range (1–4 mg mL^{-1}); in our previous work, we did not find that gelator **2d** could form a hydrogel.[44] The length of the alkyl chain is the only difference in the structure of these gelators. The results indicated that the gelation ability of these bolaamphiphiles significantly depends on the alkyl chain length. Under the same conditions of hydrogen bonding forces and π–π stacking interactions, the alkyl chain length was changed to balance the hydrophobic forces (van der Waals forces and π–π stacking forces) and hydrophilic forces (hydrogen bonding forces), which is very important for hydrogelation.[45,46] Our results show that LMWHs can be obtained by introducing different lengths of alkyl chains to finely adjust the balance of the hydrophilic and hydrophobic parts,[29] leading to the conclusion that adjusting the length of the alkyl chains is an effective way to obtain a hydrogelator.

To explore the microstructure and gelation process, different xerogel samples were observed by SEM. Since both PEG200 and PEG400 have very high boiling points (>250 °C) and low volatility, it is difficult to extract PEG from the gel *via* an oil pump at room temperature, and a xerogel was not obtained, so the gel prepared in the low boiling point solvent was selected for SEM and FT-IR characterization. All the gels have a 3D network structure and were formed by the entanglement and interweaving of fibers (Fig. 2), which indicated that the gels were formed by the self-assembly of gelators.[6,7] As the concentration of gelator **2d** increased, the diameter of the hydrogel fiber increased (Fig. 2A and B), which indicated a stronger water retention capacity. As the alkyl chain of the gelator became longer, the fiber became longer under the same concentration of gelator (Fig. 2C and D). The longer alkyl chain enhanced the van der Waals forces of gelators, which may have promoted the gelator self-assembly into longer fibers.[47]

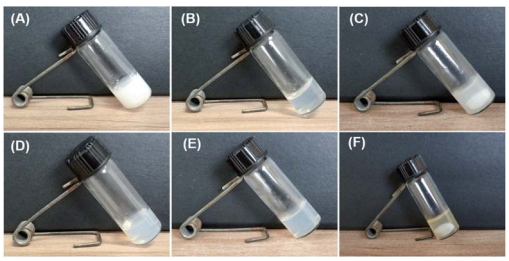

Fig. 1 Photographs of different gels. (A), (D), (E) are ethanol gels prepared by **2c** (10 mg mL^{-1}), **2e** (10 mg mL^{-1}), and **2f** (9 mg mL^{-1}) in ethanol, respectively; (B) is a hydrogel constructed by **2d** (1 mg mL^{-1}) in H_2O; (C) is the gel prepared by **2f** (9 mg mL^{-1}) in a mixed solvent of PEG200 and H_2O (v/v, 1 : 1); (F) is the levofloxacin hydrochloride-loaded gel prepared by **2f** (10 mg mL^{-1}) and levofloxacin hydrochloride (20 mg mL^{-1}) in mixture solvents of PEG200 and H_2O (v/v, 1 : 1).

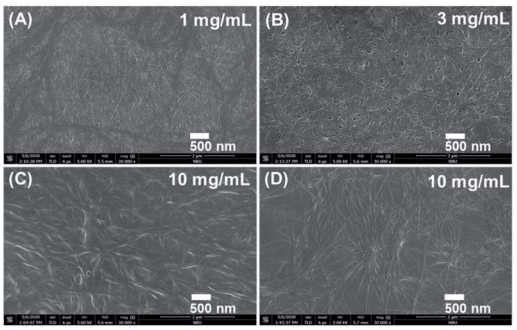

Fig. 2 SEM images of xerogels. (A) and (B) show the hydrogels of **2d** with concentrations of 1 and 3 mg mL^{-1}, respectively. (C) An ethanol gel of **2e** with a concentration of 10 mg mL^{-1}. (D) An ethanol gel of **2f** with a concentration of 10 mg mL^{-1}.

2.3 Gelation mechanism

A better understanding of the gelation mechanism is beneficial for designing the ideal gelator. FT-IR spectroscopy was used to investigate the non-covalent bond interactions of gelators in the gelation process.[43,48] In the spectrum of the gelator **2f**, the peaks at 3297.7 and 3433.8 cm^{-1} belong to the symmetrical and asymmetrical stretching vibrations of the N–H bond in the amino group, respectively (Fig. 3A). Compared with the

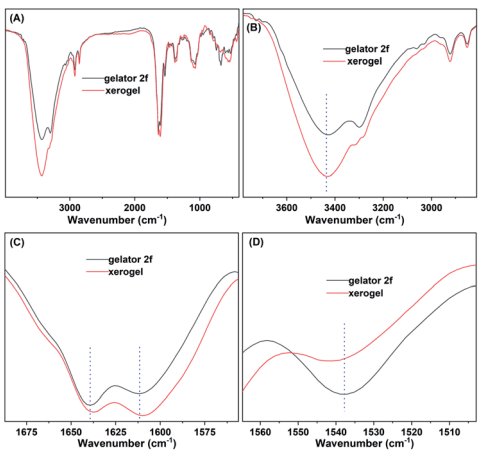

Fig. 3 Infrared spectrum (A) and locally amplified infrared spectrum (B–D) of gelator and xerogel **2f**. The xerogel was obtained by drying the ethanol gel of **2f** (10 mg mL^{-1}).

spectrum of gelator **2f**, the spectral band of the N–H stretching vibration of the xerogel was wider and stronger, and the stretching vibration frequency of the N–H bond shifted to a lower wavenumber (from 3433.8 to 3428.7 cm^{-1}) (Fig. 3A and B), which demonstrated that strong hydrogen bonding exists in the gel phase. The peaks at 2922.3 and 2852.1 cm^{-1} are characteristic of the asymmetrical and symmetrical stretching vibration peaks of methylene, respectively (Fig. 3B). The intensity of the methylene stretching vibration peak became stronger in the spectrum of the xerogel than in the spectrum of the gelator, which suggested that the alkyl chains of the gelator are in the stacked state in the gel phase. The results indicated the existence of van der Waals forces between alkyl chains.[48] The stretching vibration peaks of C=O were notably shifted to lower frequencies (from 1639.6 to 1637.1 cm^{-1}, and 1611.4 to 1608.7 cm^{-1}) (Fig. 3C), and the deformation vibration peak of N–H was markedly shifted to the higher frequency (from 1537.8 to 1541.8 cm^{-1}) (Fig. 3D), which indicated the existence of hydrogen bonding between the carbonyl group and N–H bond.[5] Similar phenomena were also observed in the comparison of hydrogel **2d** and gelator **2d**: the peak of the N–H bond became wider and stronger, the stretching vibration frequency of N–H bond shifted to lower wavenumber (from 3429.9 to 3425.2 cm^{-1}), and the intensity of the methylene stretching vibration peak became stronger (Fig. S3†). These results indicate that hydrogen bonding and van der Waals interactions are critical driving forces for both the LMOGs and LMWHs gelation processes.

To further disclose the self-assembly mechanism, the ^1H NMR spectra of gelator **2f** at different concentrations were obtained.[27] As shown in Fig. 4, the proton peaks of gelator **2f** were gradually shifted downfield with the increase in the concentration of the gelators (from 6 mg mL^{-1} to 10 mg mL^{-1}), which suggested that more gelator molecules participated in the self-assembly and the non-covalent interactions between gelators was enhanced by the increase in the concentration of the gelator. The protons on the benzene ring shifted downfield (from 7.23 to 7.29 ppm), which demonstrated there are π–π stacking interactions between the benzene ring in the gel phase.[49] Amino protons shifted downfield (from 4.58 to 4.66 ppm) with the increase in the concentration, which proved that stronger hydrogen bonding was present in the gel phase.[50] The results were probably caused by a higher percentage of gelator molecules participating in the hydrogen bonding at high concentrations, leading to a higher degree of aggregation. Methylene protons in both the alkyl chain and attached to the carbonyl markedly moved downfield (from 1.13 to 1.17, 2.16 to 2.21 ppm, respectively), which indicated that van der Waals forces are present between the alkyl chains. The above results suggest that hydrogen bonding, van der Waals forces, and π–π stacking interactions jointly drive the self-assembly of gelators.

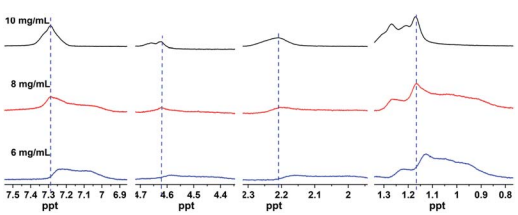

Fig. 4 ^1H NMR spectra of different concentrations of gelator **2f** in ethanol-d_6.

2.4 Rheological properties

Mechanical strength, shear thinning behavior, and the destruction–recovery ability are critical parameters of whether a gel can be used as an injectable biomaterial.[50,51] Gelators **2c** and **2e** with representative lengths of alkyl chains were chosen to investigate the rheological properties of the gels. The gels constructed by gelators **2c** and **2e** in PEG were marked as G3 and G5, respectively. As shown in Fig. 5A, the storage modulus (G') was higher than the loss modulus (G''), which demonstrated that the samples tested by rheometer are real gels.[44] The elastic modulus of G5 was higher than that of G3 under the same concentration, which indicated that with the growth of the alkyl chain, the gelation ability of the gelator was enhanced and a more stable gel was obtained. Both G3 and G5 gels exhibited shear thinning behavior (Fig. 5B). Dynamic strain and time sweep experiments demonstrated that the network structure of the gel can be destroyed by an increase in the strain and can be recovered by withdrawing the strain and extension time (Fig. 5C). This trait was endowed by the intrinsic dynamic reversible supramolecular interactions of gelators.[43,44] The G3 gel exhibited a higher mechanical strength in PEG400 than in PEG200 under the same concentration (Fig. 5D), which may have been caused by the hydrogen bonding of gelator molecules and PEG200 molecules being stronger than that of the gelator molecules and PEG400 molecules. The strong hydrogen bonding of gelator molecules and solvent molecules impaired the hydrogen bonding of the gelator molecules and led to the decreased mechanical strength of the gel. As the concentration

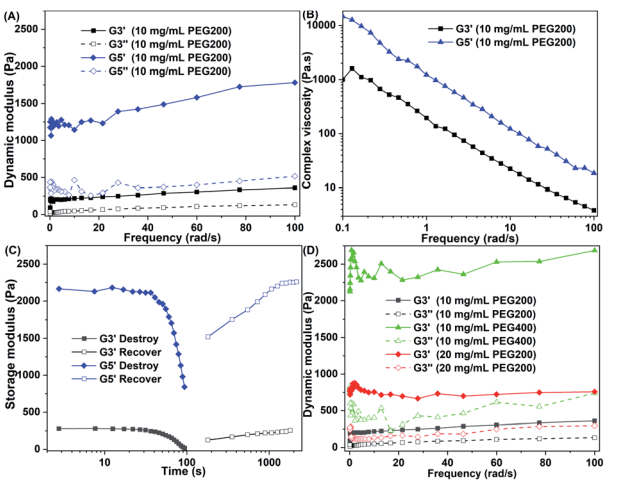

Fig. 5 Rheological properties of the gel: (A) the dynamic modulus as a function of angular frequency for gels (10 mg mL^{-1}); (B) the dynamic complex viscosity as a function of angular frequency for the gels (10 mg mL^{-1}); (C) the destruction (dynamic strain sweep) and recovery (dynamic time sweep) of gels (10 mg mL^{-1}); (D) the dynamic modulus of gels in different solvents and different concentrations as a function of angular frequency.

of the gelator increased, the mechanical strength of the gel increased (Fig. 5C), which was probably caused by a higher percentage of gelator molecules participating in self-assembly and forming thicker fibers and tighter gel networks (as shown in Fig. 2A and B). These results indicate that the mechanical strength of the gel can be enhanced by lengthening the alkyl chain in the gelator structure, increasing the concentration of the gelator, and choosing a proper solvent. Excellent shear thinning behavior and destruction–recovery ability, and appropriate mechanical strength allow this bolaamphiphile family to be used as injectable antimicrobial gels.

2.5 Antibiotic loaded gels

The properties of a compound are determined by its structure. All the gelators have similar structures that were constructed by biocompatible phenylalanine and aliphatic diacid. Gelator **2d** has good biocompatibility, which was demonstrated by our previous work.[44] The other gelators (**2a**, **2b**, **2c**, **2e**, **2f**) may have similar biocompatibility because their structures are very similar to the structure of gelator **2d**, with only a slight difference in the alkyl chain lengths. Gels constructed by these gelators in PEG200, H_2O, and a mixture of PEG200 and H_2O are biocompatible and can be used as antibiotic carriers. Photographs of the blank **2d** gel and the levofloxacin hydrochloride-loaded **2d** gel with maximum antibiotic loading are shown in Fig. S3.† The antibiotic loading contents of **2b**, **2c**, **2d**, **2e**, and **2f** were 41.2%, 41.2%, 90.9%, 50.0% and 66.7%, which were far beyond that of a nanodrug carrier. The best antibiotic loading capacity of the **2d** gel was probably due to the **2d** gelator having the best gelling performance and achieving a balance between the hydrophilicity and hydrophobicity of its structure. Hydrazide and phenylalanine moieties may also confer the gels with potential antimicrobial activity.[33,43] With shear thinning and destruction–recovery properties, these levofloxacin hydrochloride-loaded gels have huge potential application value as antimicrobial gels.

2.6 *In vitro* drug release

Phosphate buffer solution with pH 7.4 and 5.0 was chosen to study the degradation and release behavior of the gel *in vitro*.

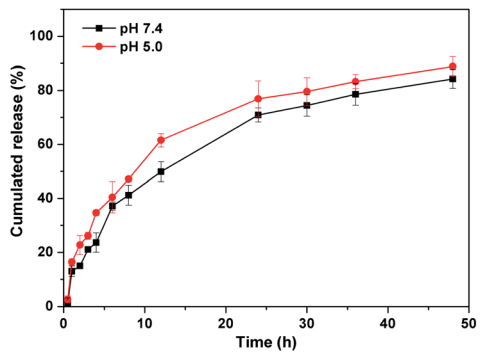

Fig. 6 Drug release profiles of levofloxacin hydrochloride-loaded **2d** gel in PBS at pH 7.4 and 5.0.

The levofloxacin hydrochloride-loaded **2d** gel at both pH 7.4 and 5.0 showed high drug release of 84.3% and 88.9%, respectively, in 48 h (Fig. 6). Since levofloxacin hydrochloride is easily soluble in water, the huge concentration difference between the gel sample and the release medium indicates that levofloxacin hydrochloride can enter into a release medium by free diffusion. The PEG200 in the gel could gradually dissolve in the medium by interface contact and lead to the gel gradually degrading to release levofloxacin hydrochloride. The faster release of the levofloxacin hydrochloride by the loaded **2d** gel under acidic conditions as compared to neutral conditions is probably due to the protonated amino group destroying the hydrophilic and hydrophobic balance of the gelator structure under acidic conditions and accelerating the degradation of the gel, leading to the effective release of the drug.

3 Experimental

3.1 Materials

All solvents and reagents used in this study were chemically pure. L-Phenylalanine methyl ester, azelaic acid, undecanedioic acid, ethanol-d_6, 1,1′-carbonyldiimidazole (CDI) and levofloxacin hydrochloride were purchased from the Saen Chemical Technology (Shanghai) Co. Ltd. Adipoyl chloride, suberoyl chloride, sebacoyl chloride, dodecanedioyl dichloride, poly(ethylene glycol) (PEG, $M_w = 200$ or 400 g mol^{-1}) were purchased from Aladdin Bio-Chem Technology (Shanghai) Co. Ltd. The solvents were purchased from Shanghai Titan Scientific Company Ltd. (China) and were used directly without further purification.

3.2 Characterization

The structures of the products were characterized by ^{1}H NMR and ^{13}C NMR spectroscopy (Bruker Avance III NMR spectrometer, Germany). The new compounds were also characterized by HRMS (Bruker solanX 70 FT-MS, Germany). The microstructures of the xerogels were observed by SEM (Magellan 3020, American). FT-IR (Nicolet 6700, American) and ^{1}H NMR spectra were used to investigate the gelation mechanism. The rheological properties of gels were investigated by a rheometer (HAAKE Rheostress 1, Germany).

3.3 The synthesis of compounds 1 (1a, 1b, 1c, 1d, 1e, 1f)

Compounds **1** (**1a**, **1b**, **1c**, **1d**, **1e**, **1f**) were prepared by a condensation reaction of L-phenylalanine methyl ester with an aliphatic diacid or aliphatic diacid chloride.[44,52] Adipoyl chloride and azelaic acid are used as examples to illustrate the synthesis and purification process of compound **1**; the other products were prepared similarly. Compound **1c**: L-phenylalanine methyl ester hydrochloride (2.26 g, 10.5 mmol) was added to dry tetrahydrofuran solution (30 mL), then triethylamine (TEA) (1.21 g, 12 mmol) was added dropwise to the solution at 0 °C with stirring for 15 min. Azelaic acid (0.94 g, 5 mmol) and CDI (1.70 g, 10.5 mmol) were dissolved in 30 mL of dry tetrahydrofuran in a separate flask, and the solution was stirred at room temperature (RT) until no bubbles were generated. The

activated acid solution was added dropwise to the mixture of L-phenylalanine methyl ester hydrochloride at 0 °C, then stirred under N_2 atmosphere for 24 h. The reaction mixture was filtered and concentrated. The residue was dissolved in dichloromethane, washed sequentially with HCl solution (1 M), saturated $NaHCO_3$ solution, saturated NaCl solution, and dried by anhydrous sodium sulfate. After the solvents were removed by rotary evaporation, the product was obtained by column chromatography (petroleum ether and ethyl acetate, v/v, 6 : 1) (yield: 90%). Compound **1a**: the hydrochloric acid molecule of L-phenylalanine methyl ester hydrochloride (2.26 g, 10.5 mmol) was removed according to the above method. Subsequently, the adipoyl chloride (1.34 g, 5 mmol) and TEA (1.06 g, 10.5 mmol) were simultaneously added through a constant pressure dropping funnel under ice bath stirring. After reacting at RT for 24 h, the reaction mixture was filtered and concentrated. The residue was dissolved in dichloromethane and washed with saturated brine, then dried by anhydrous sodium sulfate. The solvents were removed by rotary evaporation and the product was obtained by column chromatography (petroleum ether and ethyl acetate, v/v, 6 : 1) (yield: 85%).

Compound 1a. ^{1}H NMR (500 MHz, $CDCl_3$, TMS) δ 1.60 (quint, 4H, J = 3.0 Hz), 2.14–2.20 (m, 4H), 3.07 (dd, 2H, J = 6.5, 13.5 Hz), 3.15 (dd, 2H, J = 5.5, 14.0 Hz), 3.72 (s, 6H), 4.88 (dd, 2H, J = 6.5, 13.5 Hz), 6.11 (d, 2H, J = 7.5 Hz), 7.11 (d, 4H, J = 7.0 Hz), 7.22–7.30 (m, 6H). ^{13}C NMR (125 MHz, $CDCl_3$, TMS) δ (33.4, 35.2, 37.8, 52.4, 53.2, 127.2, 128.6, 129.3, 135.8, 170.5, 172.2).

Compound 1b. ^{1}H NMR (500 MHz, $CDCl_3$, TMS) δ 1.27 (br, 4H), 1.55–1.59 (m, 4H), 2.13–2.18 (m, 4H), 3.06 (dd, 2H, J = 6.0, 14.0 Hz), 3.14 (dd, 2H, J = 6.0, 14.0 Hz), 3.73 (s, 6H), 4.91 (dd, 2H, J = 6.0, 14.0 Hz), 6.00 (d, 2H, J = 7.5 Hz), 7.09 (d, 4H, J = 7.0 Hz), 7.23–7.30 (m, 6H). ^{13}C NMR (125 MHz, $CDCl_3$, TMS) δ (25.2, 36.1, 37.9, 52.3, 52.9, 127.1, 128.6, 129.2, 135.9, 172.4, 172.6).

Compound 1c. ^{1}H NMR (400 MHz, $CDCl_3$, TMS) δ 1.26 (br, 6H), 1.56–1.59 (m, 4H), 2.16 (t, 4H, J = 7.6 Hz), 3.08 (dd, 2H, J = 6.0, 13.6 Hz), 3.15 (dd, 2H, J = 6.0, 13.6 Hz), 3.73 (s, 6H), 4.90 (dd, 2H, J = 6.0, 13.6 Hz), 5.92 (d, 2H, J = 7.6 Hz), 7.09 (d, 4H, J = 7.2 Hz), 7.23–7.30 (m, 6H). ^{13}C NMR (100 MHz, $CDCl_3$, TMS) δ (25.4, 28.9, 36.4, 37.9, 52.3, 52.9, 127.1, 128.6, 129.3, 135.9, 172.2, 172.7).

Compound 1d. ^{1}H NMR (400 MHz, $CDCl_3$, TMS) δ 1.25 (br, 12H), 1.58–1.59 (m, 4H), 2.16 (t, 4H, J = 7.2 Hz), 3.08 (dd, 2H, J = 6.0, 14.0 Hz), 3.16 (dd, 2H, J = 6.0, 14.0 Hz), 3.73 (s, 6H), 4.91 (dd, 2H, J = 6.0, 13.6 Hz), 5.90 (d, 2H, J = 7.6 Hz), 7.08–7.10 (m, 4H), 7.22–7.31 (m, 6H).

Compound 1e. ^{1}H NMR (400 MHz, $CDCl_3$, TMS) δ 1.25 (br, 10H), 1.56–1.59 (m, 4H), 2.17 (t, 4H, 7.6 Hz), 3.08 (dd, 2H, J = 6.0, 14.0 Hz), 3.16 (dd, 2H, J = 6.0, 14.0 Hz), 3.73 (s, 6H), 4.90 (dd, 2H, J = 5.6, 13.6 Hz), 5.95 (d, 2H, J = 7.6 Hz), 7.08–7.10 (m, 4H), 7.22–7.31 (m, 6H). ^{13}C NMR (100 MHz, $CDCl_3$, TMS) δ (25.5, 29.1, 29.2, 36.5, 37.9, 52.3, 52.9, 127.1, 128.6, 129.2, 135.9, 172.2, 172.7).

Compound 1f. ^{1}H NMR (400 MHz, $CDCl_3$, TMS) δ 1.25 (br, 12H), 1.54–1.61 (m, 4H), 2.17 (t, 4H, 7.6 Hz), 3.09 (dd, 2H, J = 5.6, 13.6 Hz), 3.16 (dd, 2H, J = 5.6, 13.6 Hz), 3.73 (s, 6H), 4.91 (dd, 2H, J = 5.6, 13.6 Hz), 5.89 (d, 2H, J = 8.0 Hz), 7.08–7.10 (m, 4H), 7.22–7.31 (m, 6H). ^{13}C NMR (100 MHz, $CDCl_3$, TMS) δ (25.5, 29.2, 29.2, 29.3, 36.5, 37.9, 52.3, 52.9, 127.1, 128.5, 129.3, 135.9, 172.2, 172.7).

3.4 Synthesis of compounds 2 (2a, 2b, 2c, 2d, 2e, 2f)

Compounds **2a**, **2b**, **2c**, **2d**, **2e**, and **2f** were synthesized by a similar method; the synthesis of **2a** is given as an example. Compound **1a** (2.34 g, 5 mmol) and hydrazine hydrate (2 mL) were dissolved in CH_2Cl_2 and methanol (30 mL, v/v, 1 : 1). The mixture was then stirred under a N_2 atmosphere for 24 h. Subsequently, the reaction solution was filtered and the solid washed several times with dichloromethane. The gelator **2a** was obtained after vacuum drying.

Compound 2a. ^{1}H NMR (500 MHz, $CDCl_3$, TMS) δ 1.20 (br, 4H), 1.95 (br, 4H), 2.73 (dd, 2H, J = 10.0, 13.5 Hz), 2.90 (dd, 2H, J = 4.5, 13.5 Hz), 4.22 (br, 4H), 4.23–4.47 (m, 2H), 6.11 (d, 2H, J = 7.5 Hz), 7.15 (t, 4H, J = 6.5 Hz), 7.20–7.25 (m, 8H), 8.00 (d, 2H, J = 13.5 Hz), 9.20 (s, 2H). ^{13}C NMR δ (125 MHz, $CDCl_3$, TMS) δ (24.5, 34.8, 38.0, 52.4, 126.1, 128.0, 129.1, 137.9, 170.5, 171.7). HRMS (ESI^+) calcd for $(C_{24}H_{32}N_6O_4 + Na)^+$: 491.23773; found: 491.23731.

Compound 2b. ^{1}H NMR (500 MHz, $CDCl_3$, TMS) δ 0.98 (br, 4H), 1.24–1.27 (m, 4H), 1.98 (t, 4H, J = 7.5 Hz), 2.74 (dd, 2H, J = 10.0, 13.5 Hz), 2.91 (dd, 2H, J = 4.5, 13.5 Hz), 4.23 (br, 3H), 4.43–4.48 (m, 2H), 7.15–7.27 (m, 10H), 8.02 (d, 2H, J = 8.5 Hz), 9.20 (s, 2H). ^{13}C NMR (125 MHz, $CDCl_3$, TMS) δ (25.0, 28.2, 35.1, 37.9, 52.5, 126.1, 127.9, 129.1, 137.9, 170.5, 171.9). HRMS (ESI^+) calcd for $(C_{26}H_{36}N_6O_4 + Na)^+$: 519.26903; found: 519.26967.

Compound 2c. ^{1}H NMR (400 MHz, $CDCl_3$, TMS) δ 0.99–1.07 (m, 6H), 1.29–1.37 (m, 4H), 2.00 (t, 4H, J = 7.2 Hz), 2.74 (dd, 2H, J = 10.0, 13.6 Hz), 2.92 (dd, 2H, J = 4.8, 13.6 Hz), 4.30 (br, 3H), 4.43–4.49 (m, 2H), 7.15–7.29 (m, 10H), 8.03 (d, 2H, J = 8.8 Hz), 9.20 (s, 2H). ^{13}C NMR (100 MHz, $CDCl_3$, TMS) δ (25.6, 28.8, 29.0, 35.6, 38.4, 52.9, 126.6, 128.4, 129.6, 138.4, 171.1, 172.4). HRMS (ESI^+) calcd for $(C_{27}H_{38}N_6O_4 + Na)^+$: 533.28468; found: 533.28469.

Compound 2d. ^{1}H NMR (400 MHz, $CDCl_3$, TMS) δ 1.02–1.09 (m, 4H), 1.32 (quint, 4H, J = 7.2 Hz), 2.00 (t, 4H, J = 3.2 Hz), 2.73 (dd, 2H, J = 10.0, 14.0 Hz), 2.91 (dd, 2H, J = 4.8, 13.6 Hz), 4.20 (s, 4H), 4.42–4.48 (m, 2H), 7.14–7.18 (m, 2H), 7.20–7.26 (m, 8H), 8.02 (d, 2H, J = 8.4 Hz), 9.19 (s, 2H).

Compound 2e. ^{1}H NMR (400 MHz, $CDCl_3$, TMS) δ 0.98–1.05 (m, 10H), 1.26–1.39 (m, 4H), 2.00 (t, 4H, J = 6.4 Hz), 2.74 (dd, 2H, J = 10.4, 13.2 Hz), 2.91 (dd, 2H, J = 6.4, 13.2 Hz), 4.30 (br, 3H), 4.41–4.51 (m, 2H), 7.12–7.31 (m, 10H), 8.03 (d, 2H, J = 8.0 Hz), 9.21 (s, 2H). ^{13}C NMR (100 MHz, $CDCl_3$, TMS) δ (25.6, 28.9, 29.2, 29.2, 35.6, 38.4, 53.0, 126.6, 128.4, 129.6, 138.4, 171.1, 172.3). HRMS (ESI^+) calcd for $(C_{29}H_{42}N_6O_4 + Na)^+$: 561.31598; found: 561.31596.

Compound 2f. ^{1}H NMR (400 MHz, $CDCl_3$, TMS) δ 1.03–1.06 (m, 4H), 1.14 (br, 8H), 1.28–1.37 (m, 4H), 2.00 (t, 4H, J = 7.2 Hz), 2.73 (dd, 2H, J = 10.0, 13.6 Hz), 2.91 (dd, 2H, J = 4.8, 13.6 Hz), 4.22 (br, 4H), 4.42–4.48 (m, 2H), 7.15–7.26 (m, 10H), 8.03 (d, 2H, J = 8.4 Hz), 9.19 (s, 2H). ^{13}C NMR (100 MHz, $CDCl_3$, TMS) δ (25.1, 28.4, 28.8, 28.8, 35.2, 37.9, 52.4, 126.1, 127.9, 129.1, 138.0, 170.1, 171.9). HRMS (ESI^+) calcd for $(C_{29}H_{42}N_6O_4 + Na)^+$: 575.33163; found: 575.33337.

3.5 Blank gel and antibiotic-loaded gel

A given amount of gelator was added to a screw bottle, then 1 mL of solvent (PEG200, H_2O, ethanol, *etc.*) was added, and heated until completely dissolved. When cooled to RT, the solution turned into a gel. The inverted observation method was used to judge whether a gel was formed. The critical gelation concentration was obtained by testing the minimum amount of gelators required to form a stable gel. The xerogel was obtained under reduced pressure by an oil pump (Rankuum Machinery Ltd (Chengdu), type 2XZ-4B, total pressure 2.1 Pa, pumping speed 4 L s^{-1}) at RT. The xerogel was ground into a powder and placed on carbon conductive tape. After spraying with gold for 45 seconds, the microstructure of the gel was observed by scanning electron microscopy. A small amount of xerogel and potassium bromide were ground into a powder and pressed into thin sheets for infrared spectroscopic testing.

The antibiotic-loaded antimicrobial gel was prepared similarly. A certain amount of gelator and levofloxacin hydrochloride was added to a mixed solvent of H_2O and PEG200 (v/v, 1 : 1), then heated until completely dissolved. After cooling to RT, the levofloxacin hydrochloride-loaded gel was obtained. Gelators (**2b**, **2c**, **2d**, **2e**, and **2f**) with a concentration of 10 mg mL^{-1} were chosen to evaluate the antibiotic loading capacity. When the amount of added antibiotic reaches the limit for the gelator to form a gel, this critical value is the maximum antibiotic loading content. The antibiotic loading content (ALC) was calculated by the following formula:

$$\mathrm{ALC} = [\text{weight of antibiotic}/(\text{weight of antibiotic} + \text{weight of gelator})] \times 100\%$$

3.6 *In vitro* drug release profile

Levofloxacin hydrochloride-loaded **2d** gel (1 mL) with an antibiotic loading content of 50% was prepared in a 4 mL screw thread bottle as mentioned above. Then, 2 mL of phosphate buffer solution (PBS, with pH 7.4 and 5.0) was added to cover the gel and incubated at 37 °C. At the predetermined time point, 0.1 mL of release solution was taken out and 0.1 mL of fresh PBS was added. The released levofloxacin hydrochloride was measured by a microplate reader at the wavelength of 290 nm. The release experiments were conducted in 3 parallel experiments.

3.7 Rheological properties

A HAAKE Rheostress 1 was used to characterize the rheological properties of the gel, which was equipped with a temperature controller using a cone-plate geometry (diameter 35 mm). Then, 0.6 mL gel samples were added to the cone plate, the gap size was controlled at 50 μm, and the temperature was set at 25 °C. Dynamic complex viscosity (η^*), storage modulus (G'), and loss modulus (G'') were used to evaluate the viscoelastic performance of the gel. These dates were obtained by exerting an angular frequency (ω) sweep (from 0.1 to 100 rad s^{-1}) on the gel under a strain of 1.0%. Dynamic strain sweep and dynamic time sweep were used to get more information on the gel network structure. Dynamic strain sweep was applied to study the failure of the gel network structure, and the recovery properties were studied by dynamic time sweep. For dynamic strain sweep, the strain exerted on the gel samples was increased from 0.01 to 50% at 25 °C with an angular frequency of 10 rad s^{-1}. For dynamic time sweep, the strain applied on the gel samples was 0.1% with an angular frequency of 1 rad s^{-1} at 25 °C.[53]

A series of bolaamphiphiles with different alkyl chain lengths were synthesized and characterized by ^{1}H NMR and ^{13}C NMR spectra. These bolaamphiphiles (**2a**, **2b**, **2c**, **2d**, **2e**, **2f**) were efficient gelators in PEG200 and PEG400. Excitingly, due to the appropriate length of the alkyl chain, gelator **2d** was an effective hydrogelator. With their good shear thinning behavior and destruction–recovery ability, and moderate mechanical strength, the gels could be used as injectable biomaterials. The excellent antibiotic loading capacity affords these supramolecular gels great potential for application as antimicrobial gels. The results indicate that adjusting the length of the alkyl chain of bolaamphiphiles is an effective way to provide hydrogelators; due to the delicate balance of their hydrophilic and hydrophobic parts, the gelator structure can be obtained. In conclusion, our findings provide new ideas for the design of LMWHs.

Conflicts of interest

There are no conflicts to declare.

Acknowledgements

The authors thank for the financial support of Natural Science Foundation of Zhejiang Provincial (China, LQ21E030001, LQ19B020004), Foundation of Zhejiang Educational Committee (Y201839490), Natural Science Foundation of Ningbo (2019A610191), K. C. Wong Magna Fund and Research Fund (XYL20003) in Ningbo University.

Notes and references

1 J. Zhou, J. Li, X. Du and B. Xu, *Biomaterials*, 2017, **129**, 1–27.
2 S. Panja, S. Bhattacharya and K. Ghosh, *Langmuir*, 2017, **33**, 8277–8288.
3 S. Pandit, D. Dutta and S. Nie, *Nat. Mater.*, 2020, **19**, 478–480.
4 M. A. Ramin, K. R. Sindhu, A. Appavoo, K. Oumzil, M. W. Grinstaff, O. Chassande and P. Barthélémy, *Adv. Mater.*, 2017, **29**, 1605227.
5 M. Nandi, B. Maiti, S. Banerjee and P. De, *J. Polym. Sci., Part A: Polym. Chem.*, 2019, **57**, 511–521.
6 F. Mandegani, H. Zali-Boeini, Z. Khayat, J. D. Braun and D. E. Herbert, *ChemistrySelect*, 2020, **5**, 886–893.
7 L. Majumder, M. Chatterjee, K. Bera, N. C. Maiti and B. Banerji, *ACS Omega*, 2019, **4**, 14411–14419.
8 S. J. Beckers, S. Parkinson, E. Wheeldon and D. K. Smith, *Chem. Commun.*, 2019, **55**, 1947–1950.
9 H. Liu, Y. Cheng, J. Chen, F. Chang, J. Wang, J. Ding and X. Chen, *Acta Biomater.*, 2018, **73**, 103–111.
10 Y. Wang, Z. Jiang, W. Xu, Y. Yang, X. Zhuang, J. Ding and X. Chen, *ACS Appl. Mater. Interfaces*, 2019, **11**, 8725–8730.

11 K. Zheng, M. I. Setyawati, D. T. Leong and J. Xie, *Coord. Chem. Rev.*, 2018, **357**, 1–17.
12 J. Ghorbani, D. Rahban, S. Aghamiri, A. Teymouri and A. Bahador, *Laser Ther.*, 2018, **27**, 293–302.
13 K. Yang, Q. Han, B. Chen, Y. Zheng, K. Zhang, Q. Li and J. Wang, *Int. J. Nanomed.*, 2018, **13**, 2217–2263.
14 S. Li, S. Dong, W. Xu, S. Tu, L. Yan, C. Zhao, J. Ding and X. Chen, *Adv. Sci.*, 2018, **5**, 1700527.
15 T. Ghosh, A. Biswas, P. K. Gavel and A. K. Das, *Langmuir*, 2020, **36**, 1574–1584.
16 C. C. Piras, C. S. Mahon and D. K. Smith, *Chemistry*, 2020, **26**, 8452–8457.
17 Z. Zhai, K. Xu, L. Mei, C. Wu, J. Liu, Z. Liu, L. Wan and W. Zhong, *Soft Matter*, 2019, **15**, 8603–8610.
18 F. Wahid, Y. N. Zhou, H. S. Wang, T. Wan, C. Zhong and L. Q. Chu, *Int. J. Biol. Macromol.*, 2018, **114**, 1233–1239.
19 W. Zhao, Y. Li, X. Zhang, R. Zhang, Y. Hu, C. Boyer and F. J. Xu, *J. Controlled Release*, 2020, **323**, 24–35.
20 C. Zhao, L. Zhou, M. Chiao and W. Yang, *Adv. Colloid Interface Sci.*, 2020, **285**, 102280.
21 J. Wang, X. Y. Chen, Y. Zhao, Y. Yang, W. Wang, C. Wu, B. Yang, Z. Zhang, L. Zhang, Y. Liu, X. Du, W. Li, L. Qiu, P. Jiang, X. Z. Mou and Y. Q. Li, *ACS Nano*, 2019, **13**, 11686–11697.
22 E. R. Cross, S. M. Coulter, A. M. Fuentes-Caparros, K. McAulay, R. Schweins, G. Laverty and D. J. Adams, *Chem. Commun.*, 2020, **56**, 8135–8138.
23 V. R. Aldilla, R. Chen, A. D. Martin, C. E. Marjo, A. M. Rich, D. S. Black, P. Thordarson and N. Kumar, *Sci. Rep.*, 2020, **10**, 770.
24 Q. Zhao, Y. Zhao, Z. Lu and Y. Tang, *ACS Appl. Mater. Interfaces*, 2019, **11**, 16320–16327.
25 N. D. Bansode, K. R. Sindhu, C. Morel, M. Remy, J. Verget, C. Boiziau and P. Barthélémy, *Biomater. Sci.*, 2020, **8**, 3186–3192.
26 M. A. Ramin, L. Latxague, K. R. Sindhu, O. Chassande and P. Barthélémy, *Biomaterials*, 2017, **145**, 72–80.
27 S. Wu, Q. Zhang, Y. Deng, X. Li, Z. Luo, B. Zheng and S. Dong, *J. Am. Chem. Soc.*, 2020, **142**, 448–455.
28 R. Van Lommel, L. A. J. Rutgeerts, W. M. De Borggraeve, F. De Proft and M. Alonso, *ChemPlusChem*, 2020, **85**, 267–276.
29 D. Knani and D. Alperstein, *J. Phys. Chem. A*, 2017, **121**, 1113–1120.
30 L. Cohen, *Breast Dis. Year Bk. Q.*, 2009, **20**, 41.
31 H.-K. Yang, H. Zhao, P.-R. Yang and C.-H. Huang, *Colloids Surf., A*, 2017, **535**, 242–250.
32 S. Ogi, V. Stepanenko, J. Thein and F. Wurthner, *J. Am. Chem. Soc.*, 2016, **138**, 670–678.
33 L. Popiolek, *Med. Chem. Res.*, 2017, **26**, 287–301.
34 L. Popiolek, B. Rysz, A. Biernasiuk and M. Wujec, *Chem. Biol. Drug Des.*, 2020, **95**, 260–269.
35 R. Ongaratto, N. Conte, C. R. Montes D'Oca, R. C. Brinkerhoff, C. P. Ruas, M. A. Gelesky and M. G. Montes D'Oca, *New J. Chem.*, 2019, **43**, 295–303.
36 B. O. Okesola and D. K. Smith, *Chem. Commun.*, 2013, **49**, 11164–11166.
37 D. Zaguri, S. Shaham-Niv, P. Chakraborty, Z. Arnon, P. Makam, S. Bera, S. Rencus-Lazar, P. R. Stoddart, E. Gazit and N. P. Reynolds, *ACS Appl. Mater. Interfaces*, 2020, **12**, 21992–22001.
38 W. Wei, C. Luo, J. Yang, B. Sun, D. Zhao, Y. Liu, Y. Wang, W. Yang, Q. Kan, J. Sun and Z. He, *J. Controlled Release*, 2018, **285**, 187–199.
39 T. Das, M. Haring, D. Haldar and D. Diaz Diaz, *Biomater. Sci.*, 2017, **6**, 38–59.
40 L. Schnaider, S. Brahmachari, N. W. Schmidt, B. Mensa, S. Shaham-Niv, D. Bychenko, L. Adler-Abramovich, L. J. W. Shimon, S. Kolusheva, W. F. DeGrado and E. Gazit, *Nat. Commun.*, 2017, **8**, 1365.
41 A. Y. Gahane, P. Ranjan, V. Singh, R. K. Sharma, N. Sinha, M. Sharma, R. Chaudhry and A. K. Thakur, *Soft Matter*, 2018, **14**, 2234–2244.
42 A. M. Garcia, R. Lavendomme, S. Kralj, M. Kurbasic, O. Bellotto, M. C. Cringoli, S. Semeraro, A. Bandiera, R. De Zorzi and S. Marchesan, *Chemistry*, 2020, **26**, 1880–1886.
43 A. Y. Dang-i, T. Huang, N. Mehwish, X.-Q. Dou, L. Yang, V. Mukwaya, C. Xing, S. Lin and C.-L. Feng, *ACS Appl. Bio Mater.*, 2020, **3**, 2295–2304.
44 L. Xu, M. Zhao, Y. Yang, Y. Liang, C. Sun, W. Gao, S. Li, B. He and Y. Pu, *J. Mater. Chem. B*, 2017, **5**, 9157–9164.
45 L. A. Estroff and A. D. Hamilton, *Chem. Rev.*, 2004, **104**, 1201–1218.
46 M. Suzuki and K. Hanabusa, *Chem. Soc. Rev.*, 2009, **38**, 967–975.
47 A. Pal and J. Dey, *Langmuir*, 2013, **29**, 2120–2127.
48 L. Xu, Y. Hu, M. Liu, J. Chen, X. Huang, W. Gao and H. Wu, *Tetrahedron*, 2015, **71**, 2079–2088.
49 W. Hao, Q. Liu, Y. Hu, M. Liu, X. Huang, W. Gao and H. Wu, *ChemistryOpen*, 2018, **7**, 457–462.
50 L. Xu, Y. Liang, C. Sun, N. Hao, J. Yan, W. Gao and B. He, *Nanotheranostics*, 2017, **1**, 313–325.
51 J. D. Tang, E. B. Roloson, C. D. Amelung and K. J. Lampe, *ACS Biomater. Sci. Eng.*, 2019, **5**, 2117–2121.
52 A. Thalhammer, J. Mecinović and C. J. Schofield, *Tetrahedron Lett.*, 2009, **50**, 1045–1047.
53 F. Song, L.-M. Zhang, J.-F. Shi, N.-N. Li, C. Yang and L. Yan, *Mater. Sci. Eng., C*, 2010, **30**, 804–811.